


## Article

# Optimization and Experiment of Fertilizer-Spreading Device for Wheat Wide-Boundary Sowing Planter under Full Rice Straw Retention

Weiwen Luo<sup>1</sup>, Feng Wu<sup>1</sup>, Fengwei Gu<sup>2,\*</sup>, Hongbo Xu<sup>1</sup> , Gongpu Wang<sup>1</sup>, Bokai Wang<sup>1</sup>, Hongguang Yang<sup>1</sup> and Zhichao Hu<sup>1,\*</sup>

<sup>1</sup> Nanjing Institute of Agricultural Mechanization, Ministry of Agriculture and Rural Affairs, Nanjing 210014, China

<sup>2</sup> Graduate School of Chinese Academy of Agricultural Sciences, Beijing 100083, China

\* Correspondence: gufengwei@caas.cn (F.G.); huzhichao@caas.cn (Z.H.)

**Abstract:** When sowing with a wide boundary under full rice straw retention in the rice–wheat rotation area of China, conventional fertilization methods have some problems, such as a low fertilizer utilization rate, heap soil around a buried fertilizer device, or blocked fertilizing orifice. Firstly, combined with theoretical analysis, discrete element numerical simulation technology, and central composite test method, the wide-boundary fertilization device for wheat wide-boundary sowing was designed. Then, with the coefficient of variation for particle uniformity (CVPU) as the response value, the central composite experiment was carried out on the key structural parameters (focal length coefficient, lateral span, tilt angle, and ground clearance) of the wide-boundary fertilization device by EDEM software. Finally, the influential rules of core factors of the device on the CVPU were analyzed by Design-Expert software; then, the optimal parameter combination was determined and verified by a field test. The results showed that all factors had significant effects on the CVPU. The primary and secondary factors affecting the CVPU were the tilt angle, lateral span, focal length coefficient, ground clearance, tilt angle × ground clearance, and lateral span × ground clearance, in which there were certain interactions between the tilt angle and ground clearance and lateral span and ground clearance. When the focal length coefficient, lateral span, tilt angle, and ground clearance were 1.5, 60 mm, 30°, and 192 mm, respectively, the lateral was minimum. In this case, the theoretical value and field test value were 14.11% and 17.63%, respectively. The field test value is consistent with the theoretical calculation value. This study could provide references for the design of a fertilizer-spreading device with a wide boundary.

**Keywords:** agricultural machinery; rice–wheat rotation system; EDEM; wide-boundary fertilizer device



**Citation:** Luo, W.; Wu, F.; Gu, F.; Xu, H.; Wang, G.; Wang, B.; Yang, H.; Hu, Z. Optimization and Experiment of Fertilizer-Spreading Device for Wheat Wide-Boundary Sowing Planter under Full Rice Straw Retention. *Agronomy* **2022**, *12*, 2251. <https://doi.org/10.3390/agronomy12102251>

Academic Editors: Han Tang and Jinwu Wang

Received: 19 August 2022

Accepted: 14 September 2022

Published: 21 September 2022

**Publisher's Note:** MDPI stays neutral with regard to jurisdictional claims in published maps and institutional affiliations.



**Copyright:** © 2022 by the authors. Licensee MDPI, Basel, Switzerland. This article is an open access article distributed under the terms and conditions of the Creative Commons Attribution (CC BY) license (<https://creativecommons.org/licenses/by/4.0/>).

## 1. Introduction

The rice–wheat rotation system is the main farming system in the Yangtze River Delta region in China. When sowing wheat in this agronomic model, sowing should be completed 2 weeks after the rice is harvested. The sown area and yield of wheat under this agronomic model account for 20% and 22% of China's total wheat sown area and total wheat yield, respectively. It is one of the main modes of grain production in China [1,2]. However, with the background of the ban on straw burning by Chinese law and the change in China's agricultural production model, a large amount of straw has been left in the fields where wheat will be sown after the rice harvest in a rice–wheat rotation system. This kind of land is called primitive land with full rice straw (shown in Figure 1), that is, the field without any straw removal and tillage treatment after the previous rice is harvested, which has become a common phenomenon in a rice–wheat rotation area [3]. When producing wheat in primitive land with full rice straw, wheat sowing cannot be

completed on time, which leads to a reduction in yield due to a short sowing time, a large amount of straw in the field, and many production procedures [4]. Wide-boundary sowing technology with crushed straw inter-row mulching can effectively solve the above problems. This is an integrated operation of technology involving straw returning to the field and wide-boundary sowing, in which the straw is pulverized and covered on inter-rows while sowing wheat [5–7]. Meanwhile, the straw-returning mode with crushed straw inter-row mulching can maintain moisture and hinder weeds' growth, which is conducive to the implementation of conservation tillage in rice–wheat rotation areas [8–11].



**Figure 1.** Primitive land with full rice straw in rice–wheat rotation area.

International research on the technology is mainly focused on the development of straw returning to the field or sowing in a clayish–wet soil environment, but the technology of wide-boundary fertilization is rarely studied. The current fertilization methods in the sowing environment are still large-area fertilization with centrifugation or strip fertilization with ditching.

Przywara et al. [12] clarified the influence of structural and operational parameters of a centrifugal disc spreader on the spatial distribution of different physical properties of fertilizer. Hwang et al. [13] analyzed the distribution pattern of a centrifugal fertilizer distributor with two shutter holes and obtained the optimal optimum structural parameters using the discrete element method (DEM) for improved distribution uniformity. To improve the operation performance and fertilizer utilization rate of centrifugal fertilizer distributors, different scholars have studied different technologies, such as a centralized fertilizer application with an air-driven fertilizer distribution control system, the influence of key parameters of fertilizer spinner on uniformity, and the optimization of structure or working parameters [14–19]. Coetzee et al. [20] designed a deflector plate to separate the flow into two paths along the tree lines; Then, the effects of the key parameters on the spread pattern were investigated experimentally and compared to DEM results. Liu et al. [21] optimized the structural parameters of a strip-shunt plate using EDEM software and an orthogonal test. Ding et al. [22] developed dual-frequency ditching equipment which can apply starter fertilizer and base fertilizer at the same time. Additionally, they optimized the structural parameters with EDEM software. To meet the requirements of strip fertilization with ditching under different working conditions, Zhu et al. [23], Xiao et al. [24], and Du et al. [25] designed fertilization devices with different structural forms and analyzed the impact of key parameters on operation performance.

In a primitive land with full rice straw, there are many problems when using conventional methods to apply fertilizer [26,27]. Large-area fertilization using centrifugal fertilizer distributors will cause many problems, such as the need for many operations and a serious waste of fertilizer. When fertilizing with strip fertilization with ditching, it is easy for the discharge outlet of submerged components to be blocked by soil due to strong stickiness and high moisture of the soil.

To meet the demand for wide-boundary fertilization during wheat sowing on primitive land with full rice straw, combined with the working principle of wide-boundary sowing technology for crushed straw inter-row mulching, this study designed a fertilizing device for wide-boundary sowing. Combined with theoretical analysis and discrete element numerical simulation, the structure parameters of the fertilization device were optimized, and a field verification test was carried out. This study can provide a theoretical reference for the design of wheat planters applied to primitive land with full rice straw.

## 2. Structural Design and Theoretical Analysis

### 2.1. Agronomic Model of Wide-Boundary Sowing of Wheat after Rice

It is common for problems to arise—such as hanging grass on equipment, planting apparatus blockage, and low quality of covering soil—when sowing wheat by strip sowing or hole seeding due to high moisture, strong stickiness of soil, and a large amount of straw in primitive land with full rice straw. Wheat seeding with a wide boundary is a new wheat-seeding technology that combines strip and broadcasting without ridges. It has the advantages of optimizing the population structure and improving the leaf area index. Combining the working conditions of primitive land with full rice straw and the agronomic requirements for wheat seeding with a wide boundary, a sowing model with a sowing width of 240 mm and a spacing of 300 mm was proposed. It relies on a wide-boundary planter with crushed straw inter-row mulching to complete the operation. The agronomic requirements are as follows: three tasks, including crushing straw, laying straw in strips, and sowing in a wide-boundary condition, should be completed in one operation; the width of the crushed straw strip should not exceed 300 mm, and the width of the “no-straw” sowing belt between the adjacent straw belts should not be less than 240 mm. Fertilization and sowing are carried out in the full width of the 240 mm “no-straw” seeding belt, with a depth of 30–50 mm, and the post-sowing seed belt is compacted. The agronomic pattern for wide-boundary sowing of wheat after rice is shown in Figure 2.

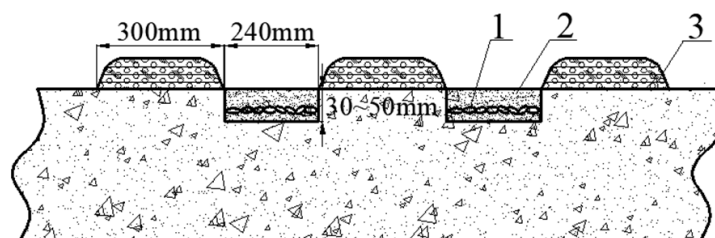


**Figure 2.** The agronomic pattern for wide-boundary sowing of wheat after rice. 1. Wheat seed. 2. “no-straw” seeding belt. 3. Straw belt.

### 2.2. Machine Structure and Working Principle

The wide-boundary planter with crushed straw inter-row mulching is mainly divided into two key processes: straw returning treatment and wheat sowing with a wide boundary. Its key operating components mainly include a straw crushing device, straw diversion device, wide-boundary fertilization device, rotary tillage device, and seeding device.

The structure of the machine is shown in Figure 3, and the main technical parameters are shown in Table 1. The working principle is as follows: the crushed straw is sprayed from the rear cover of the straw-crushing device and then divided by the straw deflector. The purpose of this process is that a “no-straw” seed strip is formed directly below the wide-boundary fertilization device, and a regular crushed straw belt is formed directly below the interval between adjacent wide-boundary fertilization devices. Meanwhile, fertilization is carried out by the wide-boundary fertilization device located under the straw deflector on the full width of the 240 mm “no-straw” seeding belt. Then, the wide-boundary seeding device carries out strip rotary plowing and wide-boundary sowing on the seeding belt covered with fertilizer. After the operation, the field showed an alternating longitudinal

arrangement of a 240 mm “no-straw” seeding belt and a 300 mm crushed straw belt. The land surface after sowing is shown in Figure 4.

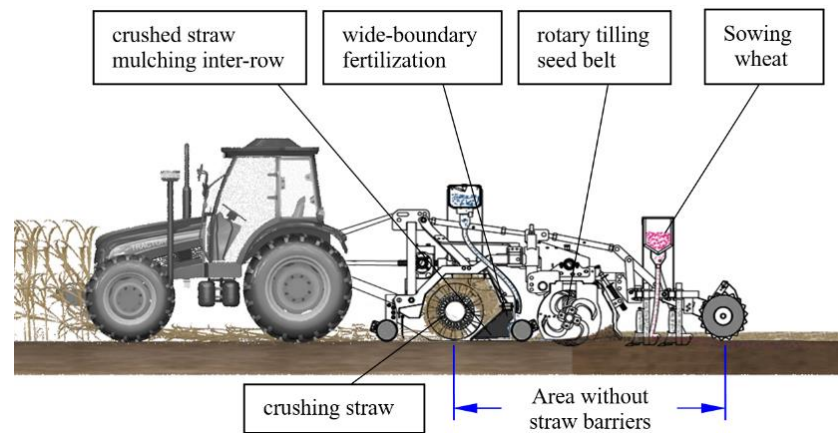


**Figure 3.** Structure of the wide-boundary planter with crushed straw inter-row mulching.

**Table 1.** Main technical parameters.

Item	Values
Overall dimension (Length × Width × High)/mm	2600 × 2400 × 1200
Weight/kg	1800
Power/kW	≥105
Velocity/(m/s)	0.8~1.8
Homework width/mm	2400
Rows	4
Covering rows	4

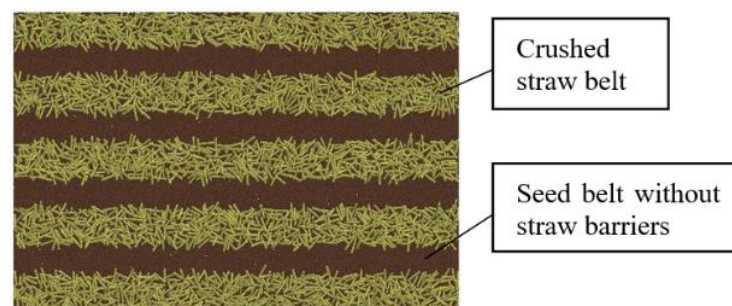


**Figure 4.** Schematic diagram of the distribution of straw belts and seeding belts on the ground after sowing.

The structure of a wide-boundary fertilization device is mainly composed of a fertilizer pipe, a fertilizer even-distribution plate, and a mounting plate. It is located directly below the crushed straw deflector, fixed on the beam after the crushing device, and corresponds to four groups of sequential crushed straw deflectors. The working principle is as follows: when fertilizers fall on the fertilizer even-distribution plate, disorderly bouncing movements occur under the blocking action of the arc plate so that the fertilizer particles are uniformly distributed laterally on the “no-straw” seed belt; at the same time, the crushed straw deflector installed outside the wide-boundary fertilization device prevents the fertilizer particles from spreading to crushed straw strips, so that all fertilizer particles fall in the “no-straw” seed belt. An assembly drawing of the crushed straw deflector and wide-boundary fertilization device is shown in Figure 5.

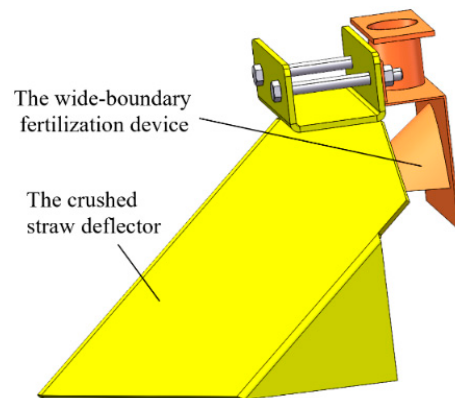


**Figure 5.** Assembly drawing of crushed straw deflector and wide-boundary fertilization device.

### 2.3. Motion Analysis of Fertilizer Particles

#### 2.3.1. Analysis of Falling Position of Fertilizer Particles

The structure of the fertilizer even-distribution plate has a crucial influence on the lateral uniformity of fertilization. When fertilizer particles collide with the fertilizer even-distribution plate, the motion trajectory is changed by the collision forces so that the fertilizer flow can be dispersed evenly. The uniform distribution performance of the fertilizer even-distribution plate with plane structure is low, which leads to an accumulation of fertilizer particles in the middle of the seeding belt. To improve the performance of the fertilizer even-distribution plate, a new even-distribution plate was designed in this study, whose cross-section is a quadratic curve and its longitudinal section is a straight line, as shown in Figure 6. Taking the intersection of the bottom surface, the symmetrical plane, and the end vertical plane of the plate as the origin, the forward direction of the machine as the positive direction of the  $y$ -axis, the vertical upward as the positive direction of the  $z$ -axis, and the right-hand rule to determine the positive direction of the  $x$ -axis, the coordinate system  $oxyz$  as shown in Figure 7 was established. The quadratic curve of the bottom surface and the straight line of the symmetrical surface satisfy Relation (1).

$$\begin{cases} x^2 = -\frac{100}{p}y + l^2 \\ z = -\tan \delta y + \frac{pl^2}{100} \tan \delta \end{cases} \quad (1)$$

where  $p$  is the focal length coefficient;  $\delta$  is the inclination angle of the device edge line in the symmetry plane,  $^\circ$ ; and  $l$  is span, mm.

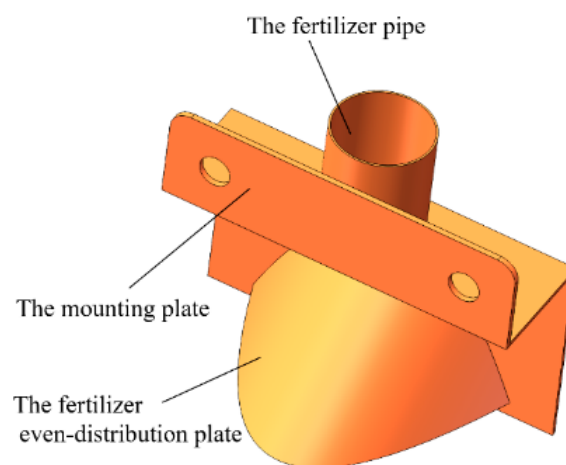


**Figure 6.** Schematic diagram of wide-boundary fertilization device.



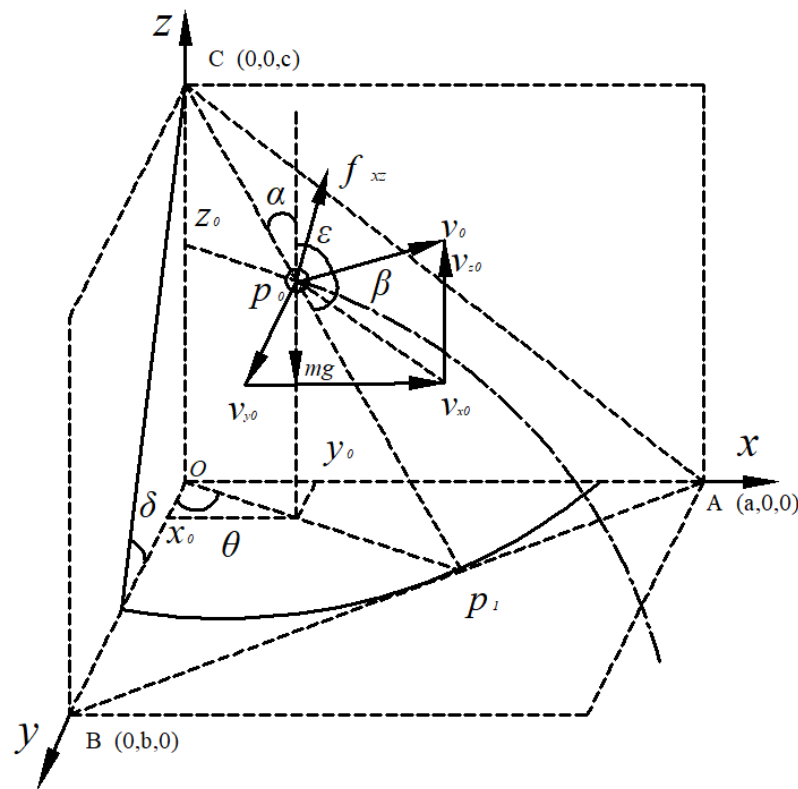


Figure 7. Schematic diagram of fertilizer particle motion analysis.

A fertilizer particle was selected as the research object, and the contact point between the particle and the fertilizer even-distribution plate is point  $p_0(x_0, y_0, z_0)$ . If the tangent plane passing through the point  $p_0$  intersects the quadratic curve at the point  $p_1(x_1, y_1, 0)$ , the following relation is established:

$$\begin{cases} y_1 = \frac{-100 + \sqrt{100^2 + 4p^2 \tan^2 \theta}}{2p \tan \theta} \\ \theta = \frac{x_0}{y_0} \end{cases} \quad (2)$$

where  $\theta$  is the angle between the projection of line  $cp_1$  on the  $xoy$  plane and the  $y$ -axis,  $^\circ$ .

$AB$  is the tangent line of the quadratic curve at point  $p_1(x_1, y_1, 0)$ , and its tangent equation is

$$y = \frac{-py_1 \tan \theta}{50}(x - y_1 \tan \theta) + y_1 \quad (3)$$

Then, the intercepts  $a$  and  $b$  of line  $AB$  on the  $x$  and  $y$  axes are, respectively:

$$\begin{cases} a = \frac{50y_1}{py_1 \tan \theta} + y_1 \tan \theta \\ b = \frac{py_1^2 \tan^2 \theta}{50} + y_1 \end{cases} \quad (4)$$

Therefore, the contact point  $p_0$  of the fertilizer particles on the fertilizer even-distribution plate satisfies the following equation:

$$\begin{cases} x_0 = \tan \theta \cdot y_0 \\ z_0 = \frac{\tan \delta p l^2}{100} \cdot \frac{ab - b \tan \theta y_0 - a y_0}{ab} \end{cases} \quad (5)$$

### 2.3.2. Fertilizer Particle Motion Analysis

Because the collision process is very short, and the collision force is much greater than gravity, friction, and air resistance, it is assumed that the displacement change of particles

and the impulse change of the above force are ignored in the theoretical analysis. According to the basic theorem of the collision process, there are the following relations:

$$\begin{cases} \frac{v_1 \sin \beta}{v_0 \sin \alpha} = e \\ v_0 \cos \alpha = v_1 \cos \beta \end{cases} \quad (6)$$

$$\begin{cases} v_1 = v_0 \cdot \sqrt{e^2 \sin^2 \alpha + \cos^2 \alpha} \\ \beta = \arcsin \frac{e \sin \alpha}{\sqrt{e^2 \sin^2 \alpha + \cos^2 \alpha}} = \arccos \frac{\cos \alpha}{\sqrt{e^2 \sin^2 \alpha + \cos^2 \alpha}} \end{cases} \quad (7)$$

where  $v_0$  is the initial velocity,  $\text{m} \cdot \text{s}^{-1}$ ;  $v_1$  is the rebound velocity,  $\text{m} \cdot \text{s}^{-1}$ ;  $\alpha$  is the angle between  $v_0$  and line  $cp_1$ , °;  $\beta$  is the angle between  $v_1$  and line  $cp_1$ , °; and  $e$  is the coefficient of restitution.

Because the machine moves at a steady speed during the operation, it is considered that the fertilizer particles are uniformly distributed longitudinally. Therefore, only the lateral homogeneity of the fertilizer granules was investigated. We can decompose the rebound velocity  $v_1$  at point  $p_0$  in the directions of the coordinate axis:

$$\begin{cases} v_{x1} = v_1 \sin(\alpha + \beta) \sin \theta \\ v_{z1} = v_1 |\cos(\pi - \alpha - \beta)| \end{cases} \quad (8)$$

where  $v_{x1}$  is the  $x$ -axis component of the initial velocity of the particle in oblique throwing motion,  $\text{m} \cdot \text{s}^{-1}$ ; and  $v_{z1}$  is the  $z$ -axis component of the initial velocity of the particle in oblique throwing motion,  $\text{m} \cdot \text{s}^{-1}$ .

The fertilizer particle performs an oblique throwing motion after bouncing at point  $p_0$ . It is assumed that the time when the fertilizer particle begins to perform oblique throwing motion is time  $t_0 = 0$ . Ignoring the spin of the particle, the differential equations of motion along the coordinate axis are established in the  $xoz$  plane.

$$\begin{cases} m \frac{d^2x}{dt^2} = -kv_x^2 \\ m \frac{d^2z}{dt^2} = -mg - (-1)^n kv_z^2 \\ f_{xy} = kv_x^2 + kv_z^2 \end{cases} \quad (9)$$

where  $v_x$  is the  $x$ -axis component of the velocity of the particle in oblique throwing motion,  $\text{m} \cdot \text{s}^{-1}$ ;  $v_z$  is the  $z$ -axis component of the velocity of the particle in oblique throwing motion,  $\text{m} \cdot \text{s}^{-1}$ ;  $m$  is the quality of fertilizer particles,  $\text{kg}$ ;  $k$  is the air resistance coefficient, which is related to the shape of the object and air density, etc. When  $v_z > 0$ ,  $n = 0$ ; when  $v_z < 0$ ,  $n = 1$ ;  $f_{xy}$  is the air resistance of the fertilizer particles on the  $xoz$  plane.

The velocity equations of the particle in the directions of the  $x$ -axis and  $z$ -axis are shown in Equation (10). The kinematic equations of the particle in the directions of the  $x$ -axis and  $z$ -axis are shown in Equation (11).

$$\begin{cases} v_x = \frac{mv_{x1}}{kv_{x1}t + m} \\ v_z = \begin{cases} \sqrt{\frac{mg}{k}} \tan[\arctan(\sqrt{\frac{k}{mg}}v_{z1} - \sqrt{\frac{gk}{m}}t)] & (0 < t < \sqrt{\frac{m}{kg}} \cdot B) \\ \sqrt{\frac{mg}{k}} \cdot \frac{-1+e^A}{1+e^A} & (t > \sqrt{\frac{m}{kg}} \cdot B) \end{cases} \end{cases} \quad (10)$$

$$\begin{cases} x = \frac{m}{k} \ln(1 + \frac{kv_{x1}t}{m}) + \tan \theta \cdot y_0 \\ z = \begin{cases} z_0 + \frac{m}{k} \ln \left\{ \frac{\cos[B - t\sqrt{\frac{kg}{m}}]}{\cos[B]} \right\} & (0 < t < \sqrt{\frac{m}{kg}} \cdot B) \\ z_0 + \ln \left\{ \frac{1}{2} + \frac{1}{2} e^{[2t\sqrt{\frac{kg}{m}} - 2B]} \right\} + t\sqrt{\frac{kg}{m}} - B & (t > \sqrt{\frac{m}{kg}} \cdot B) \end{cases} \end{cases} \quad (11)$$

Among them:

$$\begin{cases} A = 2t\sqrt{gk/m} - 2\arctan(v_{z1}\sqrt{k/mg}) \\ B = \arctan(v_{z1}\sqrt{\frac{kg}{m}}) \end{cases} \quad (12)$$

Based on the analysis of Equations (3)–(12), the following can be observed: during the entry movement of fertilizer particles, the location of the collision point is mainly related to the tilt angle and curve shape of the even-distribution plate bottom, and the falling time of particles is mainly determined by the movement path in the z-axis direction, initial velocity, and ground clearance. When the initial velocity is determined, the lateral position of particles on the ground is mainly determined by the position of the collision point and the moving time. Therefore, the focal length coefficient, lateral span, tilt angle, and ground clearance directly affect the lateral uniformity performance of the fertilizer even-distribution plate.

Through a series of single factor tests, it was preliminarily determined that the range of focal length coefficient is 0.5~1.5, the range of lateral span is 35~95 mm, the range of tilt angle is 20~50°, and the range of ground clearance is 120~260 mm.

### 3. Materials and Methods

In the process of wide-boundary fertilization, particles are subjected to the interaction force of even-distribution plate and particle flow, and the complex collision movement of particles occurs in the process. In this study, the simulation platform of fertilizer particles–device–soil tank system was built by EDEM software, and the kinematics simulation of wide-boundary fertilization process was carried out. Taking the coefficient of variation for fertilizer uniformity as the evaluation index, the influence of the core factors on operation performance was analyzed.

#### 3.1. Construction of Discrete Element Platform

The simulation model includes fertilizer particle models, device geometry models, and the statistical plate model with soil properties. Since the spherical rate of fertilizer particles is more than 90%, 4 mm spherical particles are directly used as the simulation model of fertilizer particles. The simplified model of the crushed straw deflector and the wide-boundary fertilization device was imported into EDEM software, and the statistical plate model (3000 mm × 300 mm × 20 mm) was established under the devices. The simulation platform of particle–device–statistical plate system is shown in Figure 8. Combined with [16,19], the relevant parameters of particles, devices, and statistical plate are shown in Table 2.

**Table 2.** Material property parameters of the simulation model.

Item	Fertilizer Particle	Steel	Soil Board
Density/(kg·m <sup>-3</sup> )	1380	7850	1250
Shear modulus/Pa	1.07 × 10 <sup>7</sup>	7.0 × 10 <sup>10</sup>	1.1 × 10 <sup>8</sup>
Poisson ratio	0.24	0.30	0.51
Rolling friction coefficient (interaction with fertilizer)	0.26	0.48	1.13
Static friction coefficient (interaction with fertilizer)	0.34	0.59	1.20
Restitution coefficient (interaction with fertilizer)	0.27	0.29	0.06

#### 3.2. Simulation Test Design

The operating speed of the device is generally 0.8~1.8 m/s, so the forward speed of the device and fertilizer particles–factory during the simulation process are both 1.3 m/s. The fertilizer quality required by agronomy for wheat production in the rice–wheat rotation system is 675~825 kg/hm. Combined with the simulation parameters of machine speed, the generation speed of fertilizer particles was set to 58.5 g/s. Taking focal length coefficient,



lateral span, tilt angle, and ground clearance as the test factors and the coefficient of variation for fertilizer uniformity as the response value, the compound experiment of four factors and five levels was carried out. The test factors and horizontal codes are shown in Table 3. The test schemes and results are shown in Table 4.

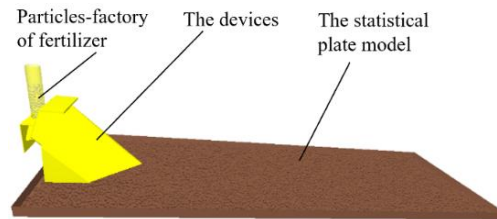


Figure 8. System model for discrete element simulation.

Table 3. Test factors and levels of virtual test.

Levels	Focal Length Coefficient	Lateral Span	Tilt Angle	Ground Clearance
−2	0.5	35	20.0	120
−1	1.0	50	27.5	155
0	1.5	65	35.0	190
1	2.0	80	42.5	225
2	2.5	95	50.0	260

Table 4. Test schemes and results.

Test Number	Focal Length Coefficient/ $X_1$	Lateral Span/ $X_2$	Tilt Angle/ $X_3$	Ground Clearance/ $X_4$	CVPU/ $Y$
1	1.0	50	27.5	155	15.46
2	1.5	65	35.0	190	17.76
3	1.0	50	42.5	225	23.92
4	1.0	80	42.5	155	27.67
5	1.0	80	42.5	225	24.93
6	2.5	65	35.0	190	25.73
7	1.5	65	35.0	190	14.71
8	2.0	80	42.5	225	27.57
9	1.5	65	35.0	260	18.28
10	2.0	50	27.5	155	17.61
11	1.5	65	35.0	190	14.44
12	1.5	95	35.0	190	24.19
13	2.0	80	42.5	155	30.08
14	1.0	50	42.5	155	25.30
15	2.0	80	27.5	155	24.57
16	1.0	50	27.5	225	20.41
17	1.5	65	35.0	120	25.46
18	1.0	50	27.5	225	18.00
19	0.5	65	35.0	190	21.95
20	1.6	65	35.0	190	16.75
21	1.0	80	27.5	225	19.56
22	2.0	80	27.5	225	21.23
23	2.0	50	42.5	225	25.64
24	1.5	65	20.0	190	18.29
25	1.5	65	50.0	190	31.00
26	2.0	50	42.5	155	28.22
27	1.5	35	35.0	190	20.08
28	1.5	65	35.0	190	16.10
29	1.0	80	27.5	155	19.71
30	1.5	65	35.0	190	15.37

### 3.3. Quality Evaluation Method for Wide-Boundary Fertilization

The forward direction of the machine is defined as longitudinal, and fertilizer is mainly distributed unevenly in the horizontal direction. Therefore, the CVPU is taken as an index to evaluate the uniformity of fertilizer application. Combined with the static test method of disc fertilizer spreader and the agronomic requirements of wide-boundary fertilization technology, the specific measurement method of CVPU is as follows: a 3000 mm strip is selected in the middle area of the statistical plate, and the Grid Bin Group module of the EDEM post-processing module is applied to divide the statistical plate into grid cells with 10 rows and 10 columns. The size of each grid cell is 300 mm × 30 mm, as shown in Figure 9. Then, the post-processing module of EDEM software was used to measure the quality of fertilizer particles in each cell. The calculation method of the CVPU is shown in Formula (13).

$$F = \frac{1}{\bar{W}} \sqrt{\frac{\sum_{i=1}^m \sum_{j=1}^n (W_{ij} - \bar{W})^2}{mn - 1}} \times 100\% \quad (13)$$

where  $F$  is the CVPU, %;  $w_{ij}$  is the mass of fertilizer particles in the grid cell in row  $i$  and column  $j$ , g.  $\bar{w}$  is the average mass of fertilizer particles in each cell, g.  $m$  is the number of rows of measurement strips.  $n$  is the number of grids for each row of strips.

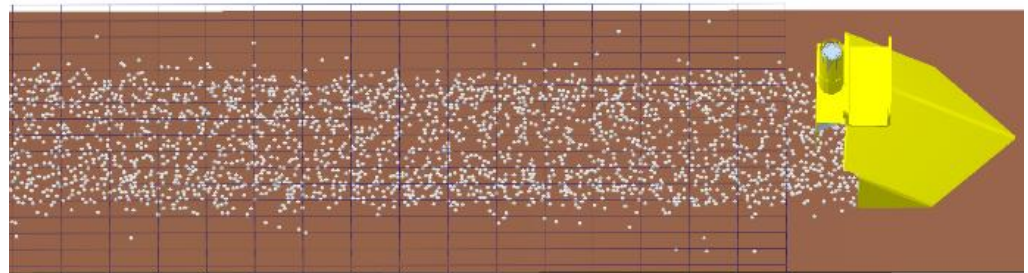


Figure 9. Schematic diagram of the data-collection grid in the sampling area.

## 4. Results and Analysis

### 4.1. Multiple Regression Analysis

The simulation test results based on the scheme are shown in Table 4. The test results are analyzed by Design-Expert software, and the model terms that are not significant are merged into the residual terms. The optimized variance analysis results are shown in Table 5. It can be seen from Table 5 that the term of the model is  $p < 0.0001$ , and the term of lack of fit is  $p = 0.5841 > 0.1$ , respectively. It is indicated that the term of the model has an extremely significant influence, and the term of lack of fit is less significant; that is, the regression model has a high degree of fit with the simulation results. The quadratic regression model is shown in Formula (14). It can be seen from Table 5 that the terms of  $X_1$ ,  $X_2$ ,  $X_3$ ,  $X_4$ ,  $X_1^2$ ,  $X_2^2$ ,  $X_3^2$ ,  $X_4^2$  have an extremely significant influence on the response value (CVPU); the term of  $X_3X_4$  has a significant influence on the response value; and the term of  $X_2X_4$  has a generally significant influence on the response value. The primary and secondary order of influence of key factors on CVPU is  $X_2 > X_1 > X_3$ .

$$Y = 15.86 + 1.18X_1 + 1.21X_2 + 3.42X_3 - 0.91X_4 - 0.63X_2X_4 - 0.69X_3X_4 + 2X_1^2 + 1.57X_2^2 + 2.2X_3^2 + 1.5X_4^2 \quad (14)$$

### 4.2. Response Surface Analysis

The response surface analysis of interaction terms in Table 5 was carried out by using Design-Expert software, as shown in Figure 10. When the focal length coefficient and tilt angle are taken as the intermediate value (1.5 and 35 mm), the interaction influence of lateral span and ground clearance on the CVPU is shown in Figure 10a. When ground clearance is determined, with the increase in the lateral span value, CVPU first decreases and then

increases; when the lateral span is determined, with the increase in ground clearance, the CVPU first decreases and then increases. When the focal length coefficient and lateral span are taken as the intermediate value (1.5 and 65 mm), the interaction influence of tilt angle and ground clearance on the CVPU is shown in Figure 10b. When the tilt angle is determined, with the increase in the ground clearance value, the CVPU first decreases and then increases; when ground clearance is determined, with the increase in the tilt angle, the CVPU first decreases and then increases.

**Table 5.** Variance analysis of regression equation.

Source	Sum of Squares	df	Mean Square	F-Value	p-Value	
Model	647.70	10	64.77	42.38	<0.0001	
X <sub>1</sub>	33.46	1	33.46	21.90	0.0002	***
X <sub>2</sub>	34.99	1	34.99	22.90	0.0001	***
X <sub>3</sub>	281.54	1	281.54	184.21	<0.0001	***
X <sub>4</sub>	19.66	1	19.66	12.86	0.0020	***
X <sub>2</sub> X <sub>4</sub>	6.40	1	6.40	4.19	0.0548	*
X <sub>3</sub> X <sub>4</sub>	7.65	1	7.65	5.00	0.0375	**
X <sub>1</sub> <sup>2</sup>	109.20	1	109.20	71.45	<0.0001	***
X <sub>2</sub> <sup>2</sup>	67.53	1	67.53	44.18	<0.0001	***
X <sub>3</sub> <sup>2</sup>	132.34	1	132.34	86.59	<0.0001	***
X <sub>4</sub> <sup>2</sup>	61.94	1	61.94	40.53	<0.0001	***
Lack of fit	20.99	14	1.50	0.93	0.5841	
Pure error	8.05	5	1.61			
Cor Total	676.74	29				

Note: \*\*\* means extremely significant ( $p < 0.01$ ), \*\* means significant ( $0.01 < p < 0.05$ ), \* means generally significant ( $0.05 < p < 0.1$ ).

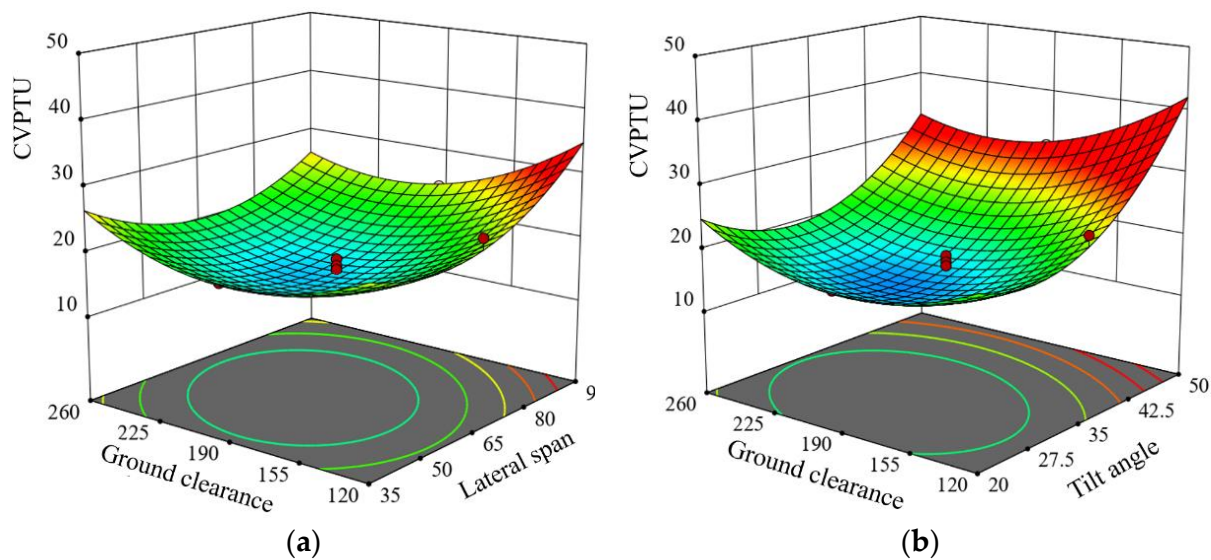


**Figure 10.** Effect of interaction between factors on CVPU. (a)  $Y = f(0, X_2, 0, X_4)$ ; (b)  $Y = f(0, 0, X_3, X_4)$ .

#### 4.3. Parameter Optimization Analysis

To optimize the operational performance of the wide-boundary fertilization device, the parameter combinations of focal length coefficient, lateral span, tilt angle, and ground clearance were optimized. The objective function and bundle function were established, as shown in Formula 15, respectively, and the mathematical model was analyzed and solved by Design-Expert software. Among a series of parameter combination schemes, the one with the highest confidence level was selected as the best parameter-combination scheme. The optimization results of parameter combination are as follows: the focal length coefficient was 1.35, the lateral span was 59.37 mm, the tilt angle was 29.21°, and the ground

clearance was 191.56 mm. In this case, the CVPU was 14.11%, and the operation effect met the relevant standards and requirements.

$$\begin{cases} \min Y(X_1, X_2, X_3, X_4) \\ s.t. \begin{cases} 0.5 \leq X_1 \leq 2.5 \\ 35 \text{ mm} \leq X_2 \leq 95 \text{ mm} \\ 20^\circ \leq X_3 \leq 50^\circ \\ 120 \text{ mm} \leq X_4 \leq 260 \text{ mm} \end{cases} \end{cases} \quad (15)$$

#### 4.4. Field Verification Test

To further verify the performance of the wide-boundary fertilization device under complex field conditions, a field test was conducted at the rice farm of Jiangsu Academy of Agricultural Sciences in October 2021. The experimental field is primitive land with full rice straw; the average height of rice straw is  $\geq 400$  mm. The type of soil is heavy, cohesive soil, and the type of fertilizer is compound fertilizer. Using the wide-boundary planter with crushed straw inter-row mulching as the test platform, field verification tests were carried out, as shown in Figure 11. The parameters of the wide-boundary fertilization device are as follows: the focal length coefficient was 1.4, the lateral span was 60 mm, the tilt angle was 30, and the ground clearance was 192 mm. During the test, the height of the rotary tillage device was adjusted upward to keep the rotary plowing knife at a certain height from the ground to avoid the interference of the rotary plowing knife on the fertilizer particles. The forward speed of the machine was set to 1.4 m/s, and the other working parameters of the machine were matched at the same time; that is, the rotational speed of the crushing device was 2000 r/min, and the rotational speed of the rotary tillage device was 300 r/min. A total of 5 repeated experiments were carried out, and the average value was taken.



**Figure 11.** Picture of field validation and test scene.

The field test results showed that the CVPU was 17.63%, and the deviation from the theoretical value and the field test value was less than 5%. The deviation was mainly caused by the poor flatness of the field ground, so the test results were basically consistent, which indicated the accuracy of the parameter's combination.

## 5. Discussions

To solve poor fertilization uniformity at low rotational speeds, Zha et al. [28] designed a blocking wheel-type screw fertilizer distributor. Simulation tests based on EDEM software were carried out to optimize the distributor variables, and then bench verification tests were built under the same conditions as the simulation tests. The results of simulation tests revealed that the minimum coefficient of variation of fertilization uniformity was 19.27%. Hwang et al. [13] analyzed the behavior of fertilizer particles on the spinner using

the discrete element method (DEM). When the optimal combination of parameters was used for the operation, the CV values were <20%. To maximize the fertilizer-utilization rate, Zhao et al. [29] designed side deep fertilizing components of a no-tillage planter. The prototype performance experiment results showed that the sowing width variation coefficient was 28.4%, which could satisfy the side deep fertilizing quality requirements. Fertilizer-application devices were extensively studied. These devices have shown good operational performance in their respective fields, with the CVPU generally being less than 30%. When the device designed in this study was used for fertilization, the field test results showed that the CVPU was 17.63%, which was consistent with the results of other related studies. The results show that it can work well under full rice straw retention.

In the case of fixed values of other factors, the CVPU first decreases and then increases with the increase in the lateral span value. The reasons for this are as follows: when the lateral span value is too small, the size of the fertilizer even-distribution plate is very small, which results in a small probability of the particles bouncing twice; so, fertilizer particles are mainly concentrated in the middle area of the seed belt. When the lateral span value is too large, the particles bounce on the fertilizer even-distribution plate many times, which leads to a larger lateral displacement of the particles; so, the distribution of the particles on the seed belt is less in the middle and more on the sides.

In the case of fixed values of other factors, the CVPU first decreases and then increases with the increase in the ground clearance value. The reasons for this are as follows: when the ground clearance value is too small, the particles' movement time in the air is too short, which leads to a small lateral displacement of particles, so the particles are concentrated in the middle area. When the ground clearance value is too large, the particles' movement time in the air is longer, which leads to a larger width of spreading fertilizer. However, under the action of the crushed straw deflector, the particles are blocked from flying out of the boundary of the seed belt. Therefore, there were more particles in the boundary and fewer particles in the middle of the seed belt.

In the case of fixed values of other factors, the CVPU first decreases and then increases with the increase in the tilt angle value. The reasons for this are as follows: when the tilt angle is too small, the number of collisions between the particles and the plate surface increases, which leads to larger velocity loss and smaller vertical velocity; therefore, the particle movement time increases, and the lateral displacement increases. When the tilt angle is too large, the incidence angle of the collision is too small, which leads to a smaller velocity change and a larger vertical velocity; so the particle motion time is shorter, which leads to insufficient lateral displacement of the particles and aggregation in the middle of the seed belt.

In addition, this study did not consider the influence of factors such as the machine operating speed, variability of fertilizer types, and particle incident speed on the CVPU, which will be further analyzed and tested in subsequent experiments. Different soil characteristics can have some influence on the field test results. On the one hand, the device designed in this study was mainly applied in the middle and lower areas of the Yangtze River plain in China, where the soil properties are more consistent. On the other hand, only representative flat plots were selected in this study to conduct multiple sets of field experiments due to the limitation of research conditions. So, the influence of soils with different characteristics on the CVPU will also be the focus of our next research.

## 6. Conclusions

Wide-boundary fertilization technology with crushed straw inter-row mulching can effectively solve the problems, such as a low fertilizer utilization rate, heap soil around a buried fertilizer device, or blocked fertilizing orifice. However, the existing scientific and technological reports are seriously deficient in the basic research and structural parameters of the wide-boundary fertilization equipment, which leads to the lack of theoretical basis in the process of production machineries. Therefore, combined with theoretical analysis and discrete element numerical simulation technology, the wide-boundary fertilization device



for wheat wide-boundary sowing was designed and systematically studied. The specific conclusions are as follows:

- (1) Aiming at the agronomic mode of wide-boundary sowing with crushed straw inter-row mulching under full straw croplands in the rice–wheat rotation system, the parameters of the wide-boundary fertilization device were designed. Through the theoretical analysis of the fertilizer movement process, it was concluded that the key structural parameters affecting the performance of the device were the focal length coefficient, lateral span, tilt angle, and ground clearance.
- (2) The central composite simulation test was conducted on the key structural parameters (focal length coefficient, span, tilt angle, and ground clearance height) with the CVPU as the response value, and the effective laws of factors on the CVPU were analyzed. The results showed that each factor has a significant effect on the CVPU, and its primary and secondary order is tilt angle, lateral span, focal length coefficient, ground clearance, tilt angle  $\times$  ground clearance, and lateral span  $\times$  ground clearance. There were certain interactions between tilt angle and ground clearance, lateral span, and ground clearance.
- (3) The parameters of the wide-boundary fertilization device were optimized. The device had better operational performance when the focal length coefficient, lateral span, tilt angle, and ground clearance were 1.4, 60 mm, 30°, and 192 mm, respectively. The simulation and field test values of the CVPU were 14.11% and 17.63%, respectively. The field test value is basically consistent with the theoretical calculation value, which verifies the accuracy of the regression model and the practical feasibility of the optimized structural parameters.

**Author Contributions:** Conceptualization, W.L. and Z.H.; methodology, F.G. and F.W.; software, H.X. and G.W.; validation, W.L. and G.W.; formal analysis, W.L. and F.G.; investigation, F.W. and G.W.; resources, B.W.; data curation, W.L.; writing—original draft preparation, W.L.; writing—review and editing, W.L.; visualization, H.X. and H.Y.; supervision, H.Y. and B.W.; project administration, Z.H.; funding acquisition, F.G. All authors have read and agreed to the published version of the manuscript.

**Funding:** This work was financially supported by the Natural Science Foundation of Jiangsu Province (grant No. BK 20221187).

**Institutional Review Board Statement:** Not applicable.

**Informed Consent Statement:** Not applicable.

**Data Availability Statement:** The data presented in this study are available in the article.

**Conflicts of Interest:** The authors declare no conflict of interest.

## References

1. Luo, W.; Gu, F.; Wu, F.; Xu, H.; Chen, Y.; Hu, Z. Design and experiment of wheat planter with straw crushing and inter-furrow collecting-mulching under full amount of straw and root stubble cropland. *Trans. Chin. Soc. Agric. Mach.* **2019**, *50*, 42–52.
2. Yang, H.; Zhai, S.; Li, Y.; Zhou, J.; He, R.; Liu, J.; Meng, Y. Waterlogging reduction and wheat yield increase through long-term ditch-buried straw return in a rice-wheat rotation system. *Field Crops Res.* **2017**, *209*, 189–197. [[CrossRef](#)]
3. Gu, F.; Hu, Z.; Chen, Y.; Wu, F. Development and experiment of peanut no-till planter under full wheat straw mulching based on “clean area planting”. *Trans. Chin. Soc. Agric. Eng.* **2016**, *32*, 15–23.
4. Luo, W.; Hu, Z.; Wu, F.; Gu, F.; Xu, H.; Chen, Y. Design and optimization for smashed straw guide device of wheat clean area planter under full straw field. *Trans. Chin. Soc. Agric. Eng.* **2019**, *35*, 1–10.
5. Xu, G.; Xie, Y.; Liang, L.; Ding, Q.; Xie, H.; Wang, J. Straw-soil-rotary blade interaction: Interactive effects of multiple operation parameters on the straw movement. *Agronomy* **2022**, *12*, 847. [[CrossRef](#)]
6. Li, Y.; Lu, C.; Li, H.; He, J.; Wang, Q.; Huang, S.; Gao, Z.; Yuan, P.; Wei, X.; Zhan, H. Design and experiment of spiral discharge anti-blocking and row-sorting device of wheat no-till planter. *Agriculture* **2022**, *12*, 468. [[CrossRef](#)]
7. Wang, B.; Gu, F.; Wu, F.; Ma, J.; Yang, H.; Hu, Z. Analysis of influencing factors and operation quality evaluation strategy of straw crushing and scattering system. *Agriculture* **2022**, *12*, 508.
8. Gu, F.; Zhao, Y.; Wu, F.; Hu, Z.; Shi, L. Simulation analysis and experimental validation of conveying device in uniform rushed straw throwing and seed-sowing Machines using CFD-DEM coupled approach. *Comput. Electron. Agric.* **2022**, *193*, 106720.



9. Shi, Y.; Xin Rex, S.; Wang, X.; Hu, Z.; Newman, D.; Ding, W. Numerical simulation and field tests of minimum-tillage planter with straw smashing and strip laying based on EDEM software. *Comput. Electron. Agric.* **2019**, *166*, 105021. [[CrossRef](#)]
10. Landers, J.N.; Freitas, P.L.D.; Oliveira, M.C.D.; Silva Neto, S.P.D.; Ralisch, R.; Kueneman, E.A. Next steps for conservation agriculture. *Agronomy* **2021**, *11*, 2496.
11. Jaskulska, I.; Romanekas, K.; Jaskulski, D.; Wojewódzki, P. A strip-till one-pass system as a component of conservation agriculture. *Agronomy* **2020**, *10*, 2015. [[CrossRef](#)]
12. Przywara, A. The impact of structural and operational parameters of the centrifugal disc spreader on the spatial distribution of fertilizer. *Agric. Agric. Sci. Procedia* **2015**, *7*, 215–222. [[CrossRef](#)]
13. Hwang, S.; Nam, J. DEM simulation model to optimise shutter hole position of a centrifugal fertiliser distributor for precise application. *Biosyst. Eng.* **2021**, *204*, 326–345. [[CrossRef](#)]
14. Lv, J.; Sun, H.; Dui, H.; Li, Z.; Li, J.; Yu, J. Optimization and Experiment of fertilizer particle motion model in conical spreading disk. *Trans. Chin. Soc. Agric. Mach.* **2018**, *49*, 85–91.
15. Liu, C.; Li, Y.; Song, J.; Ma, T.; Wang, M.; Wang, X.; Zhang, C. Performance analysis and experiment on fertilizer spreader with centrifugal swing disk based on EDEM. *Trans. Chin. Soc. Agric. Eng.* **2017**, *33*, 32–39.
16. Shi, Y.; Chen, M.; Wang, X.; Morice, O.O.; Ding, W. Design and experiment of variable-rate fertilizer spreader with centrifugal distribution cover for rice paddy surface fertilization. *Trans. Chin. Soc. Agric. Mach.* **2018**, *49*, 86–93.
17. Qi, X.; Zhou, Z.; Yang, C.; Luo, X.; Gu, X.; Zang, Y.; Liu, W. Design and experiment of key parts of pneumatic variable-rate fertilizer applicator for rice production. *Trans. Chin. Soc. Agric. Eng.* **2016**, *32*, 20–26.
18. Yang, L.; Chen, L.; Zhang, J.; Sun, H.; Liu, H.; Li, M. Test and analysis of uniformity of centrifugal disc spreading. *Trans. Chin. Soc. Agric. Mach.* **2019**, *50*, 108–114.
19. Zhang, G.; Wang, Y.; Liu, H.; Ji, C.; Hou, Q.; Zhou, Y. Design and experiments of the centrifugal side throwing fertilizer spreader for lotus root fields. *Trans. Chin. Soc. Agric. Eng.* **2021**, *37*, 37–47.
20. Coetzee, C.J.; Lombard, S.G. Discrete element method modeling of a centrifugal fertilizer spreader. *Biosyst. Eng.* **2011**, *109*, 308–325. [[CrossRef](#)]
21. Liu, J.; Gao, C.; Nie, Y.; Yang, B.; Ge, R.; Xu, Z. Numerical simulation of Fertilizer Shunt-Plate with uniformity based on EDEM software. *Comput. Electron. Agric.* **2020**, *178*, 105737.
22. Ding, S.; Bai, L.; Yao, Y.; Yue, B.; Fu, Z.; Zheng, Z.; Huang, Y. Discrete element modeling (DEM) of fertilizer dual-banding with adjustable rates. *Comput. Electron. Agric.* **2018**, *152*, 32–39.
23. Zhu, Q.; Wu, G.; Chen, L.; Zhao, C.; Meng, Z. Influences of structure parameters of straight flute wheel on fertilizing performance of fertilizer apparatus. *Trans. Chin. Soc. Agric. Eng.* **2018**, *34*, 12–20.
24. Xiao, L.; Liao, Y.; Dan, Y.; Li, M.; Wang, L.; Liao, Q. Design and experiment of quad-screw double-row fertilizer apparatus for rape seeding machine. *Trans. Chin. Soc. Agric. Mach.* **2021**, *52*, 68–77.
25. Du, X.; Liu, C.; Jiang, M.; Yuan, H.; Dai, L.; Li, F. Design and experiment of inclined trapezoidal hole fertilizer point-applied discharging device. *Trans. Chin. Soc. Agric. Mach.* **2021**, *52*, 43–53.
26. Shi, Y.; Yu, H.; Jiang, Y.; Wang, X.; Chen, H.; Liu, H. Optimization of strip fertilization planter for straw throwing and paving. *Agriculture* **2022**, *12*, 613.
27. Nourou, A.I.M.; Saidou, A.K.; Aune, J.B. Development and use of a planter for simultaneous application of seed, fertilizer and compost in pearl millet production in Niger—Effects on labor use, yield and economic return. *Agronomy* **2020**, *10*, 1886.
28. Zha, X.; Zhang, G.; Han, Y.; Salem, A.E.; Fu, J.; Zhou, Y. Structural optimization and performance evaluation of blocking wheel-type screw fertilizer distributor. *Agriculture* **2021**, *11*, 248.
29. Zhao, Y.; Wang, Y.; Gong, Z.; Yang, Y.; Zhao, S.; Gou, J. Design and experiment on side deep and layered fertilizing and seeding components of no-tillage Planter. *Trans. Chin. Soc. Agric. Mach.* **2021**, *52*, 40–50.